The Journal of Experimental Biology 215, 1266-1271
© 2012. Published by The Company of Biologists Ltd
doi:10.1242/jeb.065722

RESEARCH ARTICLE

Evaporation dynamics of tarsal liquid footprints in flies (*Calliphora vicina*) and beetles (*Coccinella septempunctata*)

Henrik Peisker* and Stanislav N. Gorb

Department of Functional Morphology and Biomechanics, Zoological Institute, Christian Albrecht University of Kiel, Am Botanischen Garten 1-9, D-24118 Kiel, Germany

*Author for correspondence (hpeisker@zoologie.uni-kiel.de)

Accepted 12 December 2011

SUMMARY

Insect tarsal adhesive structures secrete a thin layer of fluid into the contact area. It was previously reported that the presence of this fluid significantly increases adhesion on various substrata. Previous data obtained from representatives of different insect groups suggest a difference not only in the chemical composition of the fluid, but also in its physical properties. In the present study, we have measured for the first time changes in the droplet geometry over time and the evaporation rate of the fluid in flies (*Calliphora vicina*) and beetles (*Coccinella septempunctata*) by the use of atomic force microscopy. Flattened droplets of the beetle had lower evaporation rates than hemispherical footprints of the fly. Within 1 h, the droplet volume reduced to 21% of the initial volume for the fly, and to 65% for the beetle, suggesting a larger fraction of volatile compounds in the fly fluid. It was revealed that drop geometry changes significantly during evaporation and shows pinning effects for the fly footprints due to an assumed self-organizing oil layer on top of the water fraction of the micro-emulsion. The data obtained suggest that the adhesion strength in capillarity-based switchable adhesive systems must be time-dependent because of the specific evaporation rate of the adhesive fluid. These results are important for our understanding of the functional mechanism of insect adhesive systems and also for biomimetics of artificial capillarity-based adhesive systems.

Key words: atomic force microscopy, AFM, insect tarsal liquids, evaporation, wet adhesion, capillary adhesion.

INTRODUCTION

Insect adhesive organs – either smooth, soft pads or arrays of adhesive setae – have attracted the interest of scientists for more than three centuries (Hooke, 1665; Blackwall, 1830; West, 1862; Dewitz, 1884; Gorb, 1998; Niederegger et al., 2002). Owing to their structural diversity and striking mechanical performance (Beutel and Gorb, 2001), numerous experimental studies have been conducted to understand the functional principles behind specific morphological features.

It has previously been shown that in both hairy and smooth pads the contact is often mediated by an adhesive fluid (Walker et al., 1985; Ishii, 1987; Lees and Hardie, 1988; Eisner and Aneshansley, 2000; Jiao et al., 2000; Betz, 2010), which differs in chemical composition in different insect species (Gorb, 1998; Federle et al., 2002; Voetsch et al., 2002; Betz, 2010; Geiselhardt et al., 2010). In beetles, the fluid is mainly oil based, whereas in flies, it was assumed to be a water–oil micro-emulsion (Gorb, 2001). In some flies, the fluid is released through pores under the terminal spatula (Gorb, 1998), whereas for other insect species lacking such pores, the liquid transportation is provided by a system of nanoscopically small porous channels (Schwarz and Gorb, 2003). For smooth adhesive pads in stick insects, it has been demonstrated that the amount of the fluid secreted into the contact zone changes with step frequency until a non-zero steady state is reached (Dirks and Federle, 2010). Based on experiments with beetles and flies, it has been concluded that both cohesive forces and surface tension of the pad secretion have a major contribution to the mechanism of adhesion in hairy systems (Stork, 1983; Langer et al., 2004; Gorb et al., 2010). Additionally, the fluid fills cavities on rough substrates, allowing the pad to enhance contact with the surface, where a dry pad would only make limited contact (Jiao et al., 2000; Federle et al., 2002; Voetsch et al., 2002; Drechsler and Federle, 2006). That is why it is important to characterize interactions between the fluid and both the adhesive pad and the substrate. For this purpose, knowledge about physical properties of the fluid is crucial.

In some insects, the pad secretion consists of two phases: polar and non-polar (Gorb, 2001; Federle et al., 2002; Voetsch et al., 2002; Drechsler and Federle, 2006). The water-soluble part of the secretion contains carbohydrates, amino acids and proteins (Voetsch et al., 2002). The use of the lipid- and carbohydrate-containing fluid may be rather costly in the wet-adhesion-based locomotion. Regarding the amount of organic matter inside the fluid, the cost of liquid production appears to be negligible (Dirks and Federle, 2010) but when the effects of, for example, fluid deficiency are taken into account, it might be rather costly for insects to utilize wet adhesion. To estimate costs of this kind of locomotion, quantitative data on the droplet volume left behind on the surface after the footstep are required.

Despite the fact that information on the chemical composition of the attachment fluid is known for a few insect species, information on very basic properties (e.g. evaporation and viscosity) of attachment liquids in beetles and flies is still rare. The investigation of such basic processes, such as the evaporation of the adhesive fluid, is especially useful when working with these liquids (in terms of handling), and is important for discussions on the role of attachment secretions in insect adhesion.

As there seems to be a big difference in chemical composition between beetle and fly secretions, one would expect a difference in evaporation dynamics. The principal aim of this study was to investigate: (1) whether there is a significant difference in evaporation of the pad fluids of both insect species studied and (2) whether there is a change in the droplet geometry during evaporation. We measured the volume distribution, the change in radii, and the area of the liquid–air interface of footprint droplets in beetles (*Coccinella septempunctata*) and flies (*Calliphora vicina*). For this purpose, atomic force microscopy (AFM), enabling visualisation of the fluid microdroplets at a high resolution under ambient conditions, was applied. It has been previously demonstrated that this method is suitable for obtaining three-dimensional images of small droplets of liquids in the femtoliter range (Tamayo and Garcia, 1996; Herminghaus et al., 1997; Langer et al., 2004).

MATERIALS AND METHODS

Insects and footprint preparation

Five imagos of beetles [*Coccinella septempunctata* (Linnaeus 1758); Coleoptera, Coccinellidae] were captured in the botanical garden of the University of Kiel, Germany, and kept in the laboratory at 24°C and 53% relative humidity. Flies (*Calliphora vicina* Robineau-Desvoidy 1830; Diptera, Calliphoridae) were bought as larvae (Knutzen Zoo-Angel GmbH, Kiel, Germany) and raised to adults under the same laboratory conditions. Five beetles and five flies were kept for 24 h on clean moist paper towels prior to the experiments, to prevent foot contamination and desiccation.

For footprint preparation, insects were anaesthetised in a CO_2 atmosphere for 1 min. The first pair of legs was cut off using a razor blade. Immediately after separation, the ventral side of the tarsus was gently pressed on a freshly cleaved mica slide (Plano GmbH, Wetzlar, Germany) using fine forceps. By applying slight shear stress, the natural tarsal movement observed during contact formation (Niederegger and Gorb, 2003) was imitated. This manipulation resulted in the generation of the footprint, which was immediately scanned in an atomic force microscope. For beetles, only footprints of the third tarsomere of the first pair of legs were used for further quantitative analysis. Ten representative droplets per footprint of the five imagos of each species were chosen for analysis. In all, images of 100 droplets (50 droplets for beetles and 50 for flies) were analysed.

Atomic force microscopy

A NanoWizard® atomic force microscope (JPK Instruments, Berlin, Germany), mounted on an inverted light microscope (Zeiss Axiovert 135, Carl Zeiss MicroImaging GmbH, Göttingen, Germany), operating in phase contrast mode, was used for imaging. The high-frequency intermittent contact mode was applied to visualize footprints of insects. All scans were carried out in air (23°C, 43% relative humidity) with scan rates between 1.27 and 2.0 Hz and a resolution of 1024×1024 pixels with a supersharp high-frequency non-contact mode cantilever (SSS-NCH, NanoSensors, Neuchatel, Switzerland) featuring a tip curvature below 5 nm. Scan rates below 1.26 Hz as well as higher loads lead to artefacts and the smearing of droplets. These also appeared at slower oscillations of the cantilever (<340 kHz). Preliminary comparisons between droplets scanned every 15 min and droplets only scanned at t=0 min and t=60 min showed no influence of repeated measurements on droplet reduction. NanoWizard® AFM software 3.3.23 (JPK Instruments) was used to generate AFM images. Scanning probe image processing software (SPIP version 5.1.2, Image Metrology A/S, Hørsholm, Denmark) was applied to visualize and count droplets as well as measure droplet radius, height, curvature and volume.

Image processing and analysis

The irregular non-hemispherical shape of most droplets made the analysis rather complex. The variation in droplet size was determined first, to select those droplets that were in the biologically relevant range of their size distribution; fused droplets or those deposited by an incomplete contact between the seta and the substrate were not used in further analysis. Only liquid deposits belonging to the group of mean droplet volumes (see Fig. 2) were used for analysis.

Although radius, height and volume of each droplet were calculated automatically by the SPIP software module 'Particle and Pore', its liquid–air interface area was obtained manually. To ensure the correct calculation of the liquid–air interface area, A_I, droplets with a form factor of 0.85 to 1 were chosen for image analysis. The form factor provides a measure that describes the shape of a feature, where 1 corresponds to a perfect circle, and is defined by:

$$f = \frac{4\pi A}{c^2}\,, \qquad (1)$$

where A is the area calculated from the shape periphery and c is the perimeter of the droplet. The liquid–air interface area A_I of the droplet that meets the form factor constraint is then calculated with:

$$A_I = 2rh\pi\,, \qquad (2)$$

where r and h are the curvature radius and the height of the droplet, respectively.

The loss in volume over time as well as the liquid–air interface area of the droplets was analysed by applying a repeated-measures one-way ANOVA on ranks (followed by a *post hoc* Tukey's test; SigmaStat Software 3.5, Systat Software, Chicago, IL, USA). All droplets were normalized to their initial volume at t=0. This allowed a clear comparison depiction of the data.

RESULTS

Comparison of the AFM images of the footprints revealed statistically significant differences in height, ranging from 112±50 nm in the beetle to 72±50 nm in the fly (one-way ANOVA, $P \leq 0.001$). Droplets were distributed on the surface in a row-like manner, according to the distribution of the setae on the adhesive pad (Fig. 1). The diameters and the volumes of droplets, as well as their density, differed significantly between the two insect species as well as over time within each species (ANOVA, $P \leq 0.001$). Whereas the beetle droplets feature large radii (1.392±0.76 μm) and volumes (0.99±0.5 μm^3), those of the fly exhibit a denser pattern of smaller radii (0.534±0.14 μm) and volumes (0.02±0.01 μm^3; Fig. 2).

After deposition on the substrate, footprints of both insect species behaved rather differently. Droplets of *C. septempunctata* showed only a small loss in volume of ~35%, those of flies exhibited a larger volume reduction of up to ~79% during the first 60 min of observation (Figs 3–5). The difference in volume, geometry and evaporation dynamics between the two insect species is demonstrated with three-dimensional images (Fig. 4).

The decrease in volume with time is clearly visible in both species studied (Fig. 5A,B). Evaporation in *C. septempunctata* reached its highest value between 15 and 30 min and stabilised after 30 min, whereas droplets of *C. vicina* tended to evaporate slowly at the beginning. After 15 min, the fly droplets reached their highest evaporation rate.

The liquid–air interface area gives a good impression of geometrical changes and its role in evaporation dynamics. In *C. septempunctata*, the volume of the droplets changed more dramatically than the liquid–air interface area over time (Fig. 5C).

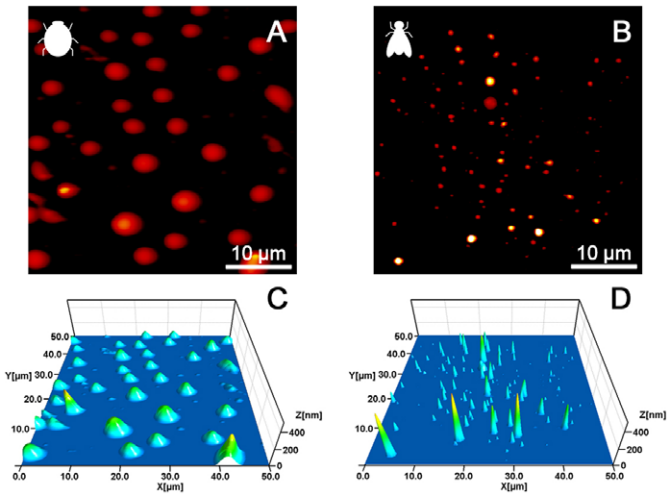

Fig. 1. Atomic force microscopy (AFM) height images of the footprint droplets of the beetle *Coccinella septempunctata* (A) and the fly *Calliphora vicina* (B) used for analysis. A and B share the same colour scale. Brighter pixels correspond to higher *z* values. (C,D) Three-dimensional impressions of the images shown in A and B, respectively.

As the interface increased because of the spreading of the droplet, the evaporation decreased. In contrast, in *C. vicina*, even though the evaporation increased, the area of the liquid–air interface decreased over time (Fig. 5D). The area of the liquid–air interface has a significant influence as it is the only interface where evaporation of the droplet can occur. The larger the interface area, the higher the evaporation rate of the droplet.

The change in droplet radius during evaporation is depicted in Fig. 5E,F. The less volatile droplets of the beetle tended to spread on the mica substrate with elapsing time (increase in the radius), whereas the more volatile fly footprints kept an almost stable radius for the first 45 min.

DISCUSSION

AFM as a tool for the characterisation of liquid–air interfaces

The high-frequency AFM method combined with the use of super sharp cantilever tips was demonstrated here to be an excellent approach to image and analyse extremely small liquid deposits, not only in non-contact mode, but also in intermittent contact mode. Any influence of the tip or repeated scanning on droplet evaporation was excluded by alternating the number of scans as well as using a check by scanning electron microscopy for a clean tip after imaging in the AFM. However, it is important to mention that the energy of the laser focused on the cantilever of the AFM may have an influence on evaporation rates. A more focused laser beam instead of the diode laser with a larger spot used here may overcome this problem. We tried to decrease the illumination time for each droplet and thus minimise the energy transmitted to the surface by using a high-speed scan approach.

Droplet form and pattern

Droplet dimensions obtained from the AFM images in the present study were comparable to values previously published for flies (Gorb, 1998) and beetles (Stork, 1983). It seems that the distribution of droplets correlates with the distribution of setae. Footprints of *C. vicina* showed a closer packing and smaller volume because of their smaller dimensions and the denser packing of the fly's setae. Furthermore, the droplets exhibited a flattened shape, which is in contrast to the hemispherical shape of water droplets on glass substrates (Gorb et al., 2010). *Coccinella septempunctata* feature larger spaces between droplets and much greater volumes of droplets. Droplets here tended to spread over the surface and therefore had large radii and low heights, as is the case for an oil-based fluid. Small droplet heights (layer thickness), essential for the generation of high capillary forces between the setae and the substrate, were found in both species studied.

Droplet geometry and evaporation dynamics

The droplet geometry measured over time clearly demonstrates a difference in the evaporation behaviour of the two tarsal liquids. The rate of evaporation in the fly fluid was much higher than that of the beetle (one-way ANOVA, $P<0.001$). On the macroscopic scale, it is known that smaller droplets tend to evaporate faster as their surface area to volume ratio increases, whereas nano droplets exhibit completely different evaporation dynamics. Droplets on the nanometer scale show a reduction in evaporation as their volume decreases when compared with a millimetre sized droplet (macroscale) of the same liquid. This has already been shown for water (Butt et al., 2007). Because of the low height of the droplets, interactions between the surface and liquid molecules are more likely (attractive forces) and thus evaporation is hindered.

Furthermore, beetle droplets feature a much larger liquid–air interface because of their flattened geometry, which should promote evaporation. Therefore, we can assume that the increased evaporation rate in the fly droplet is unlikely to be due to a large liquid–air interface. A possible explanation for the data obtained might be a higher proportion of volatile compounds in the liquid of flies (Gorb, 2001) compared with that of beetles (Betz, 2003; Geiselhardt et al., 2010).

In contrast to hydrophilic mica, we assume stronger similarity in the evaporation rates of the liquids on hydrophobic surfaces. Beetle liquid would presumably exhibit almost similar evaporation on hydrophobic surfaces because of the strong wettability and comparable spreading and contact angle of its oil-based liquid. Therefore, one would expect a similar droplet geometry and liquid–air interface compared with hydrophilic mica (Fig. 6A,C). In fly footprints, however, the liquid–air interface on a hydrophobic substrate would increase because of the higher contact angle of the liquid on the

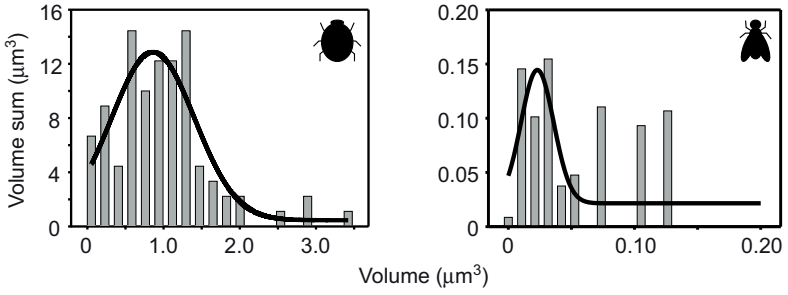

Fig. 2. Volume-weighted histograms, showing the mean droplet volumes in a footprint of the beetle *C. septempunctata* (left) and the fly *C. vicina* (right). Peaks occur at 0.986 µm³ in the beetle and 0.019 µm³ in the fly. Fifty footprints per species were used for analysis.

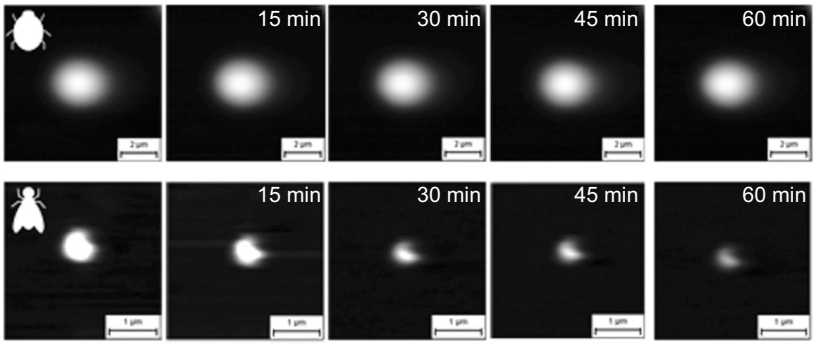

Fig. 3. AFM height images of footprint droplets of the beetle *C. septempunctata* (top) and the fly *C. vicina* (bottom) over 60 min, revealing fluid evaporation. All images corresponding to the same insect species share the same height scale: white is high, black is low.

hydrophobic substrate (Fig. 6B,D). Owing to such droplet geometry and a higher liquid–air interface, the evaporation rate should increase.

Fluid composition and evaporation dynamics

Fluids of both species exhibit a loss in volume over time (Fig. 5A,B). In the beetle, we assume that the volatile fraction of the fluid (e.g. short-chained hydrocarbons) evaporates within the first 15 to 30 min after deposition. As a result, the evaporation rate of the remaining phase (low-volatile, e.g. long-chained hydrocarbons) is lower. The stable radius in the fly droplets might be further indirect evidence for two separate phases in the liquid. We assume here that the low-volatile oily phase of the micro-emulsion tends to self-organize as a thin layer on the surface of the droplet, and thus forms a barrier shielding the volatile fraction (water) from evaporation during the first 15 min after deposition. Other authors have assumed exactly the same phenomenon and arrived at the same conclusion for another adhesive system (e.g. Betz, 2010). After 15 min, the oily fraction might be strongly depleted, exposing the water fraction to the air and promoting evaporation. Previous studies have shown a similar

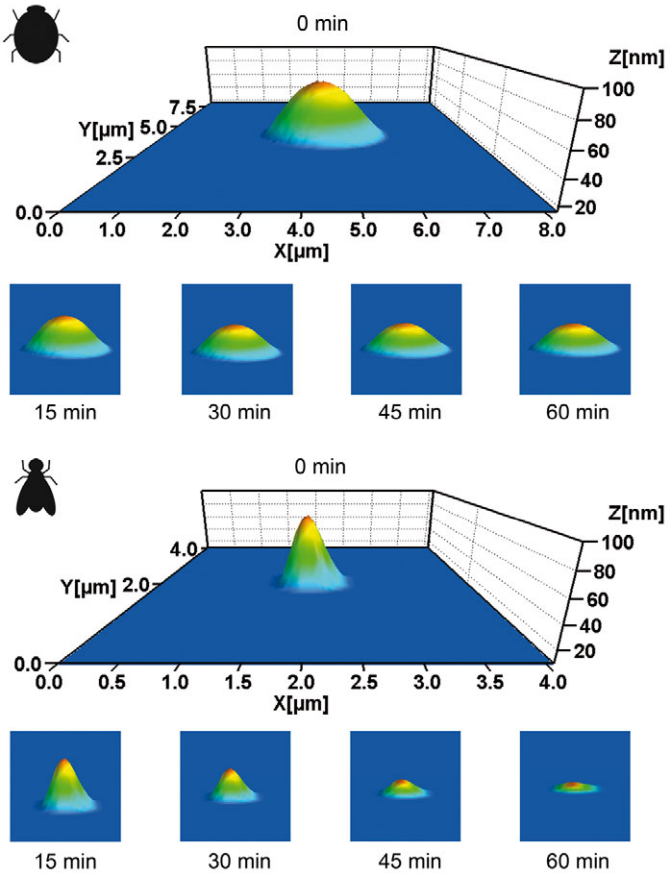

Fig. 4. Three-dimensional visualisation of the evaporation of a single droplet on mica for the beetle *C. septempunctata* (top) and the fly *C. vicina* (bottom). The difference in the evaporation rate between the two insect species is clearly visible.

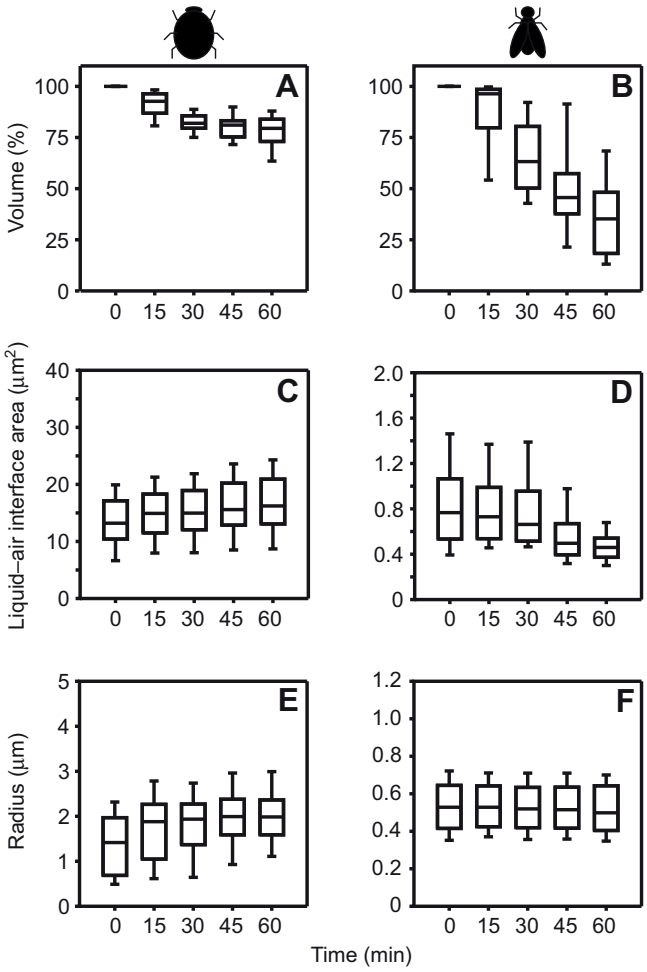

Fig. 5. Box-and-whisker plots of the volume reduction (A,B), liquid–air interface area (C,D) and radius (E,F) over time of the droplets in *C. septempunctata* (A,C,E) and *C. vicina* (B,D,F). The volume is given in percent of the initial volume of 50 individual droplets for each species, whereas the liquid–air interface area and the radii are given in absolute numbers. The ends of the boxes define the 25th and 75th percentiles, with a line at the median and error bars defining the 10th and 90th percentiles. Except for F, all parameters collected for different times are significantly different within one plot (repeated-measures one-way ANOVA on ranks, $P<0.001$).

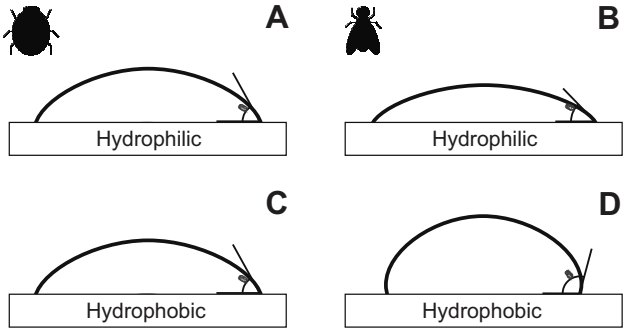

Fig. 6. Schematic of the assumed droplet behaviour and change in contact angle on hydrophilic and hydrophobic substrates for footprints of the beetle *C. septempunctata* (A,C) and the fly *C. vicina* (B,D). Differences in chemical composition is an assumed factor leading to differences in droplet geometry and various evaporation dynamics on hydrophilic and hydrophobic surfaces. Beetle footprints are assumed to evaporate at similar rates, as they have similar wettabilities and liquid–air interface areas on both surfaces. In contrast, fly footprints contain a larger water fraction and presumably have a larger contact angle and liquid–air interface area on hydrophobic surfaces. Thus, there is a greater difference in evaporation rate and dynamics of the geometry change between hydrophilic and hydrophobic surfaces for the fly. Please note that droplets are not drawn to scale.

effect in the evaporation dynamics of emulsions, which was described as 'pinning' of liquids (de Gennes, 1985; Decker and Garoff, 1997; Deegan, 2000). In order to explain the obtained AFM data in the present study, the assumed evaporation dynamics of the single droplet of the oil-based liquid of the beetle and the pinning effect of the water–oil emulsion of the fly are depicted in Fig. 7. Because the evaporation rate of beetle droplets is rather low, one may assume that the beetle fluid is very viscous, but recent data on the Colorado potato beetle *Leptinotarsa decemlineata* indicate that fluid viscosity is only slightly higher than that of water (Abou et al., 2010). We assume that *C. septempunctata* has a similar fluid viscosity; however, this remains unknown for this species. A slightly higher viscosity of the fluid could enable the beetle to utilize viscous adhesion for locomotion (Abou et al., 2010). Furthermore, the slow evaporation rate of the liquid facilitates long-term adherence without the necessity of re-establishing the contact and, therefore, may contribute to an enhanced control of attachment. Additionally, when the insect stays in contact with the substrate, such a slow evaporation minimizes the necessary amount of rather costly fluid associated with locomotion based on wet adhesion. However, during fast locomotion, when fluid loss depends on the amount of liquid left on the substrate, evaporation might be of minor relevance.

Possible role of fluid evaporation dynamics of pad fluid in insect biology

As previously assumed, the properties of secreted tarsal liquids may also play an important role in prey capture because of the high wettability of the oily part of the fluid to the cuticle surfaces of other arthropods (Betz and Kölsch, 2004). An oil–water mixture would also enable insects to attach to a variety of different surfaces, similarly well to both hydrophilic and hydrophobic ones, during terrestrial locomotion (Betz and Kölsch, 2004). One could assume that the beetles used in the present study can regulate fluid production depending on the environment and the current adhesion demands.

In the dry attachment systems of geckos and spiders, humidity in the range of 60–80% has been found to be responsible for the observed increase in adhesion (Huber et al., 2005; Wolff and Gorb, 2011). Interestingly, the time spent in dry environments has only a negligible effect on the changes in attachment ability of the Colorado potato beetle over time (Voigt et al., 2010). Our findings support this result, showing a very low evaporation rate of the beetle fluid. Additionally, the evaporation of the liquid is further reduced in

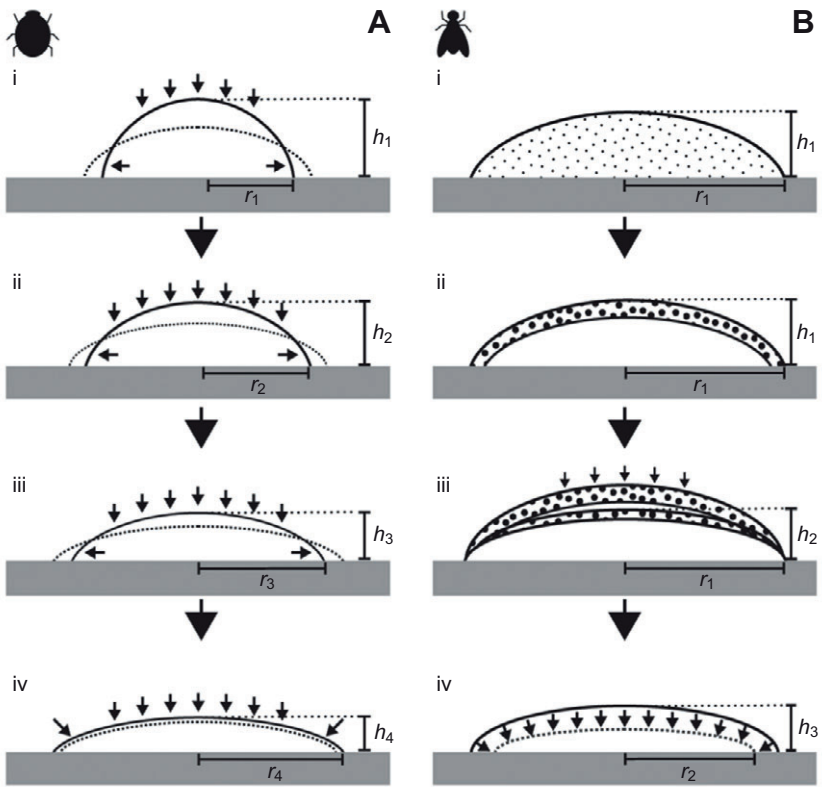

Fig. 7. Schematic illustration of the assumed evaporation dynamics of beetle (A) and fly (B) footprint droplets based on the performed AFM experiments. (A) Within the first 30 min after footprint deposition, the beetle droplet experiences a steady reduction in height (h_1>>h_2>>h_3), while the radius increases (r_1<r_2<r_3<r_4) and the volume decreases rather quickly (i–iii). After 45 min, the volume reaches a stable state with a low evaporation rate (h_3>h_4) (iv). (B) Droplet of the fly directly after deposition, with the oil fraction of the emulsion indicated by dots (i). The oil fraction presumably accumulates and forms a layer (large dots) on the top of the water fraction of the fluid, and reduces evaporation rate and droplet spreading (ii). During evaporation, the droplet first experiences only a small reduction in height (h_1) with constant droplet radius (pinning of the contact line). With time, the oil layer vanishes slowly (iii). When oil layer thickness becomes strongly reduced, the water fraction of the emulsion starts to evaporate faster (h_1>>h_2>>h_3). Droplet radius r_1 decreases to r_2, the pinning stops, and the interface moves (in the diagram, this is indicated by the change from the solid line to the dashed line). Droplets are not drawn to scale. Arrows indicate the movement of the fluid–air interface.

beetles, because only a small liquid–air interface is present when the setae are in contact with the substrate. In this situation, evaporation occurs only at the meniscus circumference.

Biomimetic potential

The ability of insect tarsal liquids to wet surfaces, as well as their rather slow evaporation behavior (especially in *C. septempunctata*) in combination with their comparably low viscosity (Abou et al., 2010), is certainly of interest for some technical adaptations, i.e. the lubrication of micro-electro-mechanical systems to prolong the lifetime of such devices. Additionally, femtoliter droplet sizes at the tips of patterned adhesives could lead to increased adhesion strength in capillarity-based adhesive systems, which have been previously described in the literature (Vogel and Steen, 2010; Kovalev and Gorb, 2011).

ACKNOWLEDGEMENTS

Valuable discussions with Lars Heepe and Alexander Kovalev on fluid mechanics and statistics are acknowledged.

FUNDING

This work, as part of the European Science Foundation EUROCORES Programme FANAS, was supported from funds by the German Science Foundation (contract no. GO 995/4-1) and the EC Sixth Framework Programme (contract no. ERAS-CT-2003-980409) to S.N.G.

REFERENCES

Abou, B., Gay, C., Laurent, B., Cardoso, O., Voigt, D., Peisker, H. and Gorb, S. (2010). Extensive collection of femtolitre pad secretion droplets in the beetle *Leptinotarsa decemlineata* allows nanolitre microrheology. *J. R. Soc. Interface* **7**, 1745-1752.

Betz, O. (2003). Structure of the tarsi in some *Stenus* species (Coleoptera, Staphylinidae): external morphology, ultrastructure, and tarsal secretion. *J. Morphol.* **255**, 24-43.

Betz, O. (2010). Adhesive exocrine glands in insects: morphology, ultrastructure, and adhesive secretion. In *Biological Adhesive Systems. From Nature to Technical and Medical Application* (ed. J. Byern and I. Grunwald), pp. 111-152. New York: Springer.

Betz, O. and Kölsch, G. (2004). The role of adhesion in prey capture and predator defence in arthropods. *Arthropod Struct. Dev.* **33**, 3-30.

Beutel, R. G. and Gorb, S. N. (2001). Ultrastructure of attachment specializations of hexapods (Arthropoda): evolutionary patterns inferred from a revised ordinal phylogeny. *J. Zool. Syst. Evol. Res.* **39**, 177-207.

Blackwall, J. (1830). Remarks on the pulvilli of insects. *Trans. Linn. Soc.* **16**, 487-492.

Butt, H. J., Golovko, D. S. and Bonaccurso, E. (2007). On the derivation of Young's equation for sessile drops: nonequilibrium effects due to evaporation. *J. Phys. Chem. B* **111**, 5277-5283.

de Gennes, P. G. (1985). Wetting: statics and dynamics. *Rev. Mod. Phys.* **57**, 827.

Decker, E. L. and Garoff, S. (1997). Contact line structure and dynamics on surfaces with contact angle hysteresis. *Langmuir* **13**, 6321-6332.

Deegan, R. D. (2000). Pattern formation in drying drops. *Phys. Rev. E* **61**, 475-485.

Dewitz, H. (1884). Ueber die Fortbewegung der Thiere an senkrechten, glatten Flächen vermittelst eines Secretes. *Eur. J. Physiol.* **33**, 440-481.

Dirks, J.-H. and Federle, W. (2010). Mechanisms of fluid production in smooth adhesive pads of insects. *J. R. Soc. Interface* **8**, 952-960.

Drechsler, P. and Federle, W. (2006). Biomechanics of smooth adhesive pads in insects: influence of tarsal secretion on attachment performance. *J. Comp. Physiol. A* **192**, 1213-1222.

Eisner, T. and Aneshansley, D. J. (2000). Defense by foot adhesion in a beetle (*Hemisphaerota cyanea*). *Proc. Natl. Acad. Sci. USA* **97**, 6568-6573.

Federle, W., Riehle, M., Curtis, A. S. G. and Full, R. J. (2002). An integrative study of insect adhesion: mechanics and wet adhesion of pretarsal pads in ants. *Integr. Comp. Biol.* **42**, 1100-1106.

Geiselhardt, S. F., Federle, W., Prüm, B., Geiselhardt, S., Lamm, S. and Peschke, K. (2010). Impact of chemical manipulation of tarsal liquids on attachment in the Colorado potato beetle, *Leptinotarsa decemlineata*. *J. Insect Physiol.* **56**, 398-404.

Gorb, E. V., Hosoda, N., Miksch, C. and Gorb, S. N. (2010). Slippery pores: anti-adhesive effect of nanoporous substrates on the beetle attachment system. *J. R. Soc. Interface* **7**, 1571-1579.

Gorb, S. (2001). *Attachment Devices of Insect Cuticle*: New York: Springer.

Gorb, S. N. (1998). The design of the fly adhesive pad: Distal tenent setae are adapted to the delivery of an adhesive secretion. *Proc. R. Soc. Lond. B* **265**, 747-752.

Herminghaus, S., Fery, A. and Reim, D. (1997). Imaging of droplets of aqueous solutions by tapping-mode scanning force microscopy. *Ultramicroscopy* **69**, 211-217.

Hooke, R. (1665). *Micrographia*. London.

Huber, G., Gorb, S. N., Spolenak, R. and Arzt, E. (2005). Resolving the nanoscale adhesion of individual gecko spatulae by atomic force microscopy. *Biol. Letters* **1**, 2-4.

Ishii, S. (1987). Adhesion of a leaf feeding ladybird *Epilachna vigintioctomaculta* (Coleoptera: Coccinellidae) on a vertically smooth surface. *Appl. Entomol. Zool.* **22**, 222-228.

Jiao, Y., Gorb, S. and Scherge, M. (2000). Adhesion measured on the attachment pads of *Tettigonia viridissima* (Orthoptera, insecta). *J. Exp. Biol.* **203**, 1887-1895.

Kovalev, A. and Gorb, S. N. (2011). Can fluid enhance adhesion of a microstructured polymer? In *Proceedings of the 34th Annual Meeting of the Adhesion Society*. Savannah, GA: Adhesion Society.

Langer, M. G., Ruppersberg, J. P. and Gorb, S. (2004). Adhesion forces measured at the level of a terminal plate of the fly's seta. *Proc. R. Soc. Lond. B* **271**, 2209-2215.

Lees, A. D. and Hardie, J. I. M. (1988). The organs of adhesion in the aphid *Megoura viciae*. *J. Exp. Biol.* **136**, 209-228.

Niederegger, S. and Gorb, S. (2003). Tarsal movements in flies during leg attachment and detachment on a smooth substrate. *J. Insect Physiol.* **49**, 611-620.

Niederegger, S., Gorb, S. and Jiao, Y. K. (2002). Contact behaviour of tenent setae in attachment pads of the blowfly *Calliphora vicina* (Diptera, Calliphoridae). *J. Comp. Physiol. A* **187**, 961-970.

Schwarz, H. and Gorb, S. (2003). Method of platinum-carbon coating of ultrathin sections for transmission and scanning electron microscopy: an application for study of biological composites. *Microsc. Res. Tech.* **62**, 218-224.

Stork, N. E. (1983). The adherence of beetle tarsal setae to glass. *J. Nat. Hist.* **17**, 583-597.

Tamayo, J. and Garcia, R. (1996). Deformation, contact time, and phase contrast in tapping mode scanning force microscopy. *Langmuir* **12**, 4430-4435.

Voetsch, W., Nicholson, G., Muller, R., Stierhof, Y. D., Gorb, S. and Schwarz, U. (2002). Chemical composition of the attachment pad secretion of the locust *Locusta migratoria*. *Insect Biochem. Mol. Biol.* **32**, 1605-1613.

Vogel, M. J. and Steen, P. H. (2010). Capillarity-based switchable adhesion. *Proc. Natl. Acad. Sci. USA* **107**, 3377-3381.

Voigt, D., Schuppert, J. M., Dattinger, S. and Gorb, S. N. (2010). Temporary stay at various environmental humidities affects attachment ability of Colorado potato beetles *Leptinotarsa decemlineata* (Coleoptera, Chrysomelidae). *J. Zool.* **281**, 227-231.

Walker, G., Yule, A. B. and Ratcliffe, J. (1985). The adhesive organ of the blowfly, *Calliphora vomitoria* – a functional approach (Diptera, Calliphoridae). *J. Zool.* **205**, 297-307.

West, T. (1862). The foot of the fly, its structure and action elucidated by comparison with the feet of other insects. *Trans. Linn. Soc.* **23**, 393-421.

Wolff, J. O. and Gorb, S. N. (2011). The influence of humidity on the attachment ability of the spider *Philodromus dispar* (Araneae, Philodromidae). *Proc. R. Soc. Lond. B* **279**, 139-143.